



Interferometric Measurements with Wideband Signal Processing Techniques

Jitendra Singh, Cornel Ioana, Matt Geen, Jerome I. Mars

► To cite this version:

Jitendra Singh, Cornel Ioana, Matt Geen, Jerome I. Mars. Interferometric Measurements with Wideband Signal Processing Techniques. OCEANS 2019 - OCEANS '19 MTS/IEEE. Let's sea our future together, Jun 2019, Marseille, France. hal-02398754

HAL Id: hal-02398754

<https://hal.science/hal-02398754>

Submitted on 7 Dec 2019

HAL is a multi-disciplinary open access archive for the deposit and dissemination of scientific research documents, whether they are published or not. The documents may come from teaching and research institutions in France or abroad, or from public or private research centers.

L'archive ouverte pluridisciplinaire **HAL**, est destinée au dépôt et à la diffusion de documents scientifiques de niveau recherche, publiés ou non, émanant des établissements d'enseignement et de recherche français ou étrangers, des laboratoires publics ou privés.

Interferometric Measurements with Wideband Signal Processing Techniques

Jitendra Singh Sewada
Univ. Grenoble Alpes, CNRS,
Grenoble INP*, GIPSA-Lab,
38000 Grenoble, France
*Institute of Engineering Univ.
Grenoble Alpes
jitendra-singh.sewada@gipsa-
lab.grenoble-inp.fr

Cornel Ioana
Univ. Grenoble Alpes, CNRS,
Grenoble INP*, GIPSA-Lab,
38000 Grenoble, France
*Institute of Engineering Univ.
Grenoble Alpes
Cornel.Ioana@gipsa-
lab.grenoble-inp.fr

Matt Geen
ITER Systems
310 Impasse de la Tuilerie,
74410 Saint-Jorioz, France
matt.geen@iter-systems.com

Jérôme Mars
Univ. Grenoble Alpes, CNRS,
Grenoble INP*, GIPSA-Lab,
38000 Grenoble, France
*Institute of Engineering Univ.
Grenoble Alpes
jerome.mars@gipsa-
lab.grenoble-inp.fr

Abstract— Bathymetric sonar systems are widely used nowadays in seafloor mapping and exploration. The differential phase technique, also known as interferometry, is widely used in these bathymetry measurement sonars, but the assessment of measurement uncertainty and data density are not completely understood and explored. This research paper concerns the description of measurement uncertainties due to different noise sources in interferometric sonars and a wideband signal processing approach to solve them. Interferometers are mostly used in shallow waters, e.g. lakes, inland waterways, rivers, reservoirs and coastal areas, due to having wider swaths compared to conventional multibeam echosounders or beamformers. This paper focuses on getting high-resolution bathymetry with minimum measurement uncertainty. It considers the effect of various acoustic noise sources, and neglects external error sources, e.g. INS, GNSS, sound velocity profiles. Wideband pulses are now used to overcome the range-resolution trade off problem of CW pulses. We have done an assessment of wideband signal processing techniques to reduce the bathymetry uncertainties caused by different noise sources. ITER Systems provided us with a Bathyswath-2 bathymetry system and essential surveying tools. Mathematical noise models are compared with data recorded in the field.

Keywords—Bathymetric sonar, Phase Differential Bathymetry Sonar, PDBS, Interferometer, Wideband signals, Matched Filters, Pulse compression, Bottom estimation, Swath bathymetry, Sonar resolution

I. INTRODUCTION

Bathymetry surveys have long been a big part of underwater exploration for commercial or non-commercial interests. There has been lot of work done to improve underwater surveying equipment, but the view underwater is still not clear, so there is a need for high-resolution and highly accurate seabed maps and 3D images. Bathymetric survey tools include sidescan sonar, single-beam echosounder, multibeam echosounder, interferometers, etc. Multibeam echosounders (MBES) and interferometers are widely used for bathymetry measurements and use beamforming and phase differing bathymetry measurement techniques respectively. Both have their advantages and disadvantages, depending on the surveying environment. Interferometers are preferred in shallow water, where wide swath range is desired, and MBES (beamformers)

are widely used in deeper water. Interferometers and MBES use different range and angle measurement techniques. An MBES measures range for beams at known angle, and an interferometer measures angle for each range.

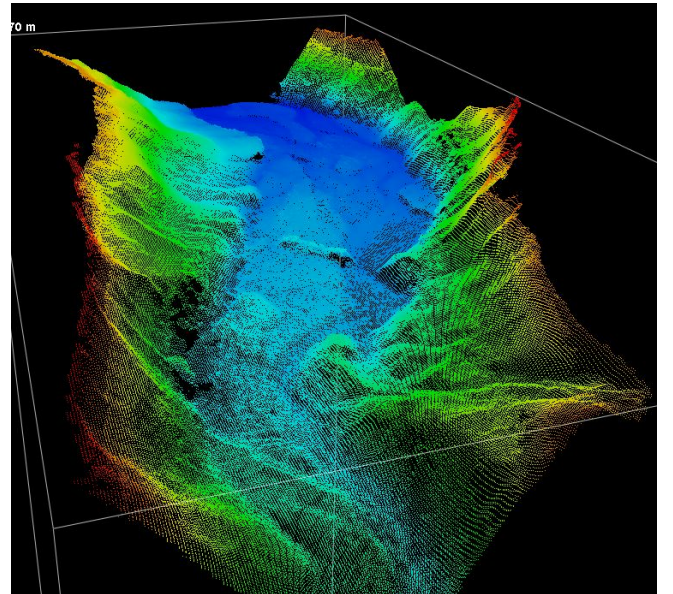


Figure 1 Digital Terrain Model (DTM) created using an interferometer

The interferometric method is currently less preferred in the hydrographic community, due to higher measurement uncertainties, but we believe that the interferometric technique holds lots of potential in shallow water surveying. We focus here on the study of different bathymetry degradation sources and possible improvements using wideband signal processing techniques.

We give a quick introduction to the interferometric method of bathymetry measurement, and the problems it faces. Section II analyses the different sources of measurement uncertainty with and without wideband signals. It then suggests ideas for further developments. Section III proposes a method to improve the overall measurement accuracy.

A. Interferometers: Measurement Techniques

The use of the word “interferometry” in sonar systems comes from the initial use of interference patterns in sidescan images to estimate the angle of incidence of seabed backscattered echoes at transducer face, known as Lloyd mirror effect [1]. Measurements with this technique are limited and highly inaccurate, as they rely on a flat sea bed and a calm sea surface.

Recent interferometers use a different approach than the linear process of adding two or more signals to get an interference pattern. The phase difference in backscattered signals at two or more closely spaced receivers is used to calculate the angle of arrival. P. Denbigh coined the term “Bathymetric sidescan sonar (BASS)” to describe the phase differencing technique [2].

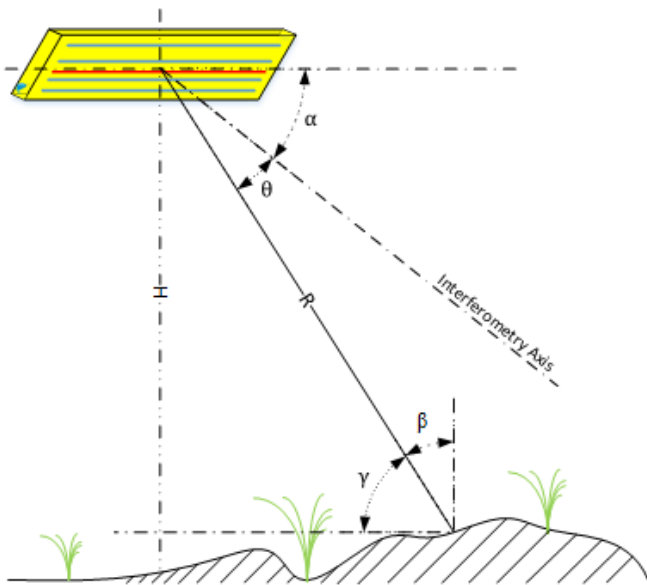


Figure 2 Basic Setup of Interferometry Sonar Transducer

The angle of arrival can be written as:

$$\theta = \sin^{-1} \left(\frac{\Delta\phi \lambda}{d} \right) \quad (1)$$

where $\Delta\phi$ is the measured phase difference between two signals of λ wavelength at two receivers separated by distance d .

The phase difference of the interferometry term can be given by:

$$\Delta\phi = \arg\{S_a S_b^*\} \quad (2)$$

where S_a and S_b are the complex signals measured at the two receivers

For this paper all the measurements were done in shallow water in Lake Annecy, France. A Bathyswath-2 transducer, supplied by ITER Systems, was used on a fixed platform with minimal motion. The average depth under the transducer was 1.5m and lake bottom was mostly flat with fine sediments. The centre frequency of transducer was 234kHz with around 100 kHz bandwidth. A complete interferometric system consists of a dual transducer set looking to both port and starboard sides [3].

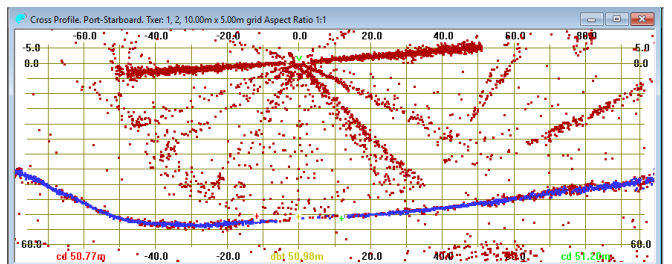


Figure 3 Spread of depth over horizontal range measured with dual transducer setup looking port and starboard sides

II. BATHYMETRY MEAURMENT UNCERTAINTIES

The source of bathymetry measurement uncertainty is a combination of errors in time of arrival measurement and angle of arrival estimation. A depth measurement error can be written as:

$$\frac{\delta H}{H} = \frac{\delta t}{t} + \tan(\theta) . \delta\theta \quad (3)$$

This paper only considers the angle measurement uncertainty $\delta\theta$. In the first section we talk about the range-resolution trade-off to understand the need for wideband signals and later we discuss the different noise sources separately. It is relatively very easy to obtain accurate timing measurements in electronic systems.

A. Range -Resolution Trade-off: need for wideband signals

Conventional systems use continuous wave (CW) pulses due to simplicity and reliable accuracy. But CW systems face a high trade-off between range and resolution. To achieve a longer slant-range, a higher energy transmit envelope is desired, which can be achieved by increasing the transmit amplitude and the transmit pulse length. The transmitted energy of a square envelope can be given by:

$$E_e = A^2 T \quad (4)$$

Where A is the transmit signal's amplitude, which is limited by the physical parameters of transducer and the power amplifier design. A longer transmitted pulse length T gives a longer slant range, but at the cost of the spatial resolution of the system. Range resolution of an imaging sonar for rectangular transmitted pulses is given approximately by $\Delta r \cong 0.59 (cT/2)$, if the target response is measured by the -3dB bandwidth, and $\Delta r = cT/2$, for a matched filter output. A higher frequency system has higher resolution, but range is limited due to higher propagation loss in water.

To overcome this problem, pulse compression techniques are used. This is done by using a frequency modulated transmitted signal and then correlating the backscattered echoes to the stored replica of the transmitted signal. Theoretically, this should allow us to increase the pulse length as much as required, while keeping the same resolution.

Figure 4 shows results from a water tank experiment with different transmitted pulses, e.g. continuous wave (CW), linear frequency modulated (LFM) and exponential frequency modulated (EFM) pulses. A ladder shaped target with two rungs

was placed in front of a transducer with 234kHz center frequency.

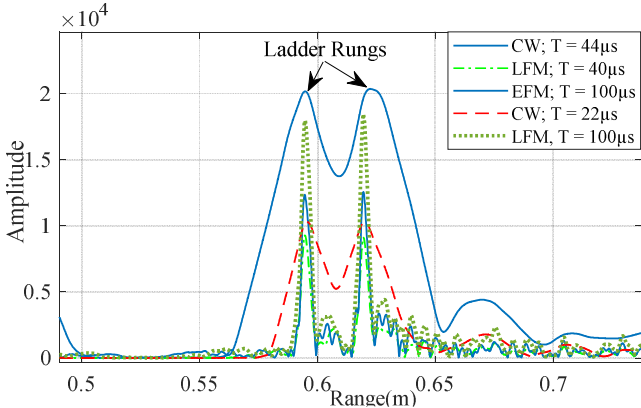


Figure 4 Matched filter output of backscattered echoes with CW, LFM & EFM transmitted pulses

A 100 μ s LFM pulse gives the same resolution as a 4.6 μ s CW pulse, with a higher signal to noise ratio (SNR). The EFM pulse gives slightly lower SNR but the resolution is same as LFM. So, from the range resolution trade-off point of view there is no added benefit from using EFM pulses. Now the pulse length T is given by the width of main lobe of the matched filter output, which is given by the bandwidth of the transmitted wideband signal. Hence, the range resolution is given by $\Delta r \approx c/(2 \times B)$, where B is the bandwidth of transmitted pulse. The frequency of the wideband signal is commonly set by the linear modulation function (LFM).

The aim of using wideband signals is to increase the signal to noise ratio while keeping high spatial resolution, but the bathymetry measurements it gives are nosier than using short CW pulses, due to baseline decorrelation, as explained in next section.

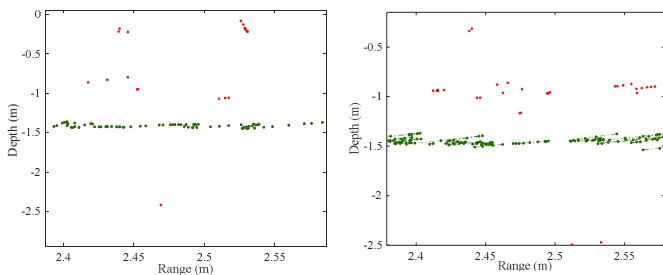


Figure 5 Sea bottom measured with transmitted CW and LFM pulses

B. Angle measurements

Interferometry, or the phase differencing technique, can be done using just one pair of receiver transducers, but the interferometry equation (1) has major problem of phase ambiguity, as discussed in this section.

I) Phase Ambiguity: Vernier Method

The first issue with the interferometry technique is the ambiguity in phase difference measurements. The receive array separation, also known as the “baseline” plays an important role in the measurement accuracy.

- Ambiguous Measurements: If the receive arrays are separated by more than one wavelength of the signal then the measured phase difference wraps around at least once, so a given phase difference corresponds to more than one angle of arrival.
- Measurement Accuracy: A smaller baseline ($<\lambda/2$) gives unambiguous angle measurement but the phase to angle curve is very shallow, which returns a highly uncertain angle value for a measured phase difference.

Figure 6 clearly represents the phase ambiguity problem when the baseline is bigger than the half wavelength ($>\lambda/2$), and for shallower phase to angle ramp for smaller separations. A Vernier pair ($\lambda/2$) is unambiguous and covers a $-\pi$ to $+\pi$ range.

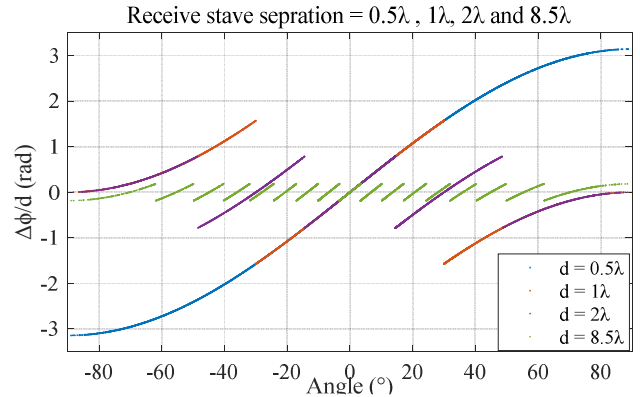


Figure 6 Phase Difference between resulting virtual pair of 0.5λ , 1λ and Physical receiver pair separated by 2λ and 8.5λ as a function of angle of incidence

The problem of phase ambiguity can be resolved using the Vernier method [5]. The idea is to create an artificial receiver pair by subtracting the phase difference measurements of two pairs. We did a successive computation of phase to angle calculation starting from the Vernier pair ($\lambda/2$) to maximum physical separation (8.5λ), obtaining an accurate angle of arrival. Figure 7 gives a good example of Vernier computation to unwrap the ambiguous angle measurements (in red).

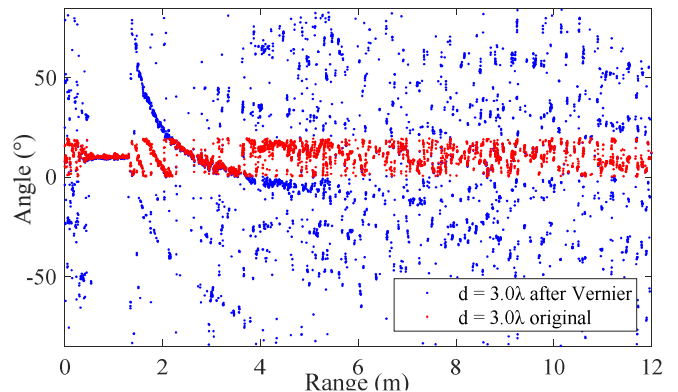


Figure 7 Angle vs Slant range; ambiguous angle (Red) & unwrapped angle (Blue)

2) Angle measurement errors

Disregarding the phase ambiguity and all the external measurement uncertainties (i.e. motion accuracy, sound velocity measurement accuracy, navigation system accuracy...), the final bathymetry measurement accuracy depends on the accuracy of angle measurement from the phase difference measurements. We describe below the major sources of noise that are responsible for the overall bathymetry degradation and which can be directly related to signal processing techniques.

a) Additive noise

Additive noise is a combination of different noise sources from the sonar itself and the propagation environment. The signal to noise only considering additive noise can be given by the active sonar equation:

$$SNR = SL - 2TL - TS - NL + DI + PG \quad (5)$$

Where:

- **SL:** Source Level is transmitted energy level and can be given by:

$$SL = S_v + 20 \log_{10}(V_{rms}) \quad (6)$$

Where S_v is the transmit channel's sensitivity

- **DI:** Directivity Index is the measure of the fraction of sound energy that is emitted in the desired direction.

$$DI_e = 20 \log_{10} \left(\frac{P_{1m}(\theta, \psi)}{P_{iso1m}} \right) \quad (7)$$

- **TL:** Transmission Loss can be given as a combination of geometric spreading and propagation loss.

$$TL \approx 20 \log_{10} R + \alpha R \quad (8)$$

Where α is the absorption coefficient and R is propagation range.

- **TS:** Target Strength is the portion of energy backscattered towards the sonar receivers:

$$TS = 10 \log_{10} \left(\frac{I_r}{I_i} \right) \quad (9)$$

- **PG:** Processing Gain is the improvement in the signal to noise ratio of the received signal by the sonar system. It could include front-end amplifiers and filter gains. For a matched filter it can be given as:

$$PG = 10 \log_{10}(BT) \quad (10)$$

- **NL:** Noise Level consists of self-noise, ambient noise and interferences. NL highly depends on the centre frequency and bandwidth of the system.

$$NL = NL_0 + 10 \log_{10} B \quad (11)$$

From the sonar equation (5), the additive noise can be directly related to the transmitted energy and the propagation loss. As discussed in the previous section, a wideband signal with pulse compression can help to increase the signal to noise ratio (SNR) contributed by additive noise. Figure 8 shows a

significant increase in the SNR using an LFM transmitted pulse over a CW pulse. Both are given from the matched filter output, so the range resolution stays high even with a long LFM pulse.

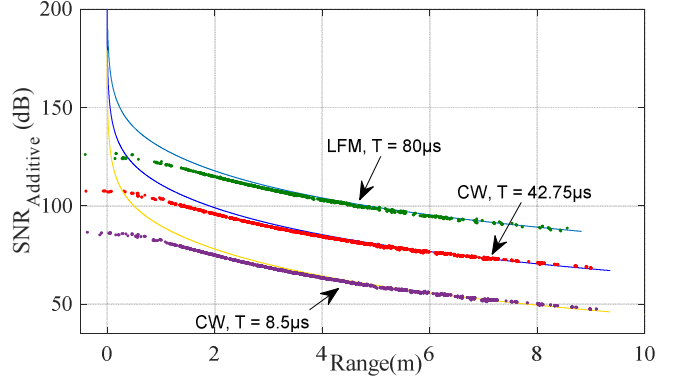


Figure 8 Additive SNR (dB) given over the horizontal range (meters) with CW (Pink) and LFM (green) transmitted pulse. Both model (solid) and field data (dotted) are presented

b) Sliding Footprint (Spatial Decorrelation)

The footprint on the seabed seen by two different receivers at a given time is slightly shifted, resulting in decorrelation between the received signals, giving increased uncertainties in the final bathymetry measurements. This phenomenon is known as spatial decorrelation or the sliding ladder (SL) effect in some literature. This decorrelation is directly related to the grazing angle (γ), pulse duration (T), and the transducer's receive array separation (D).

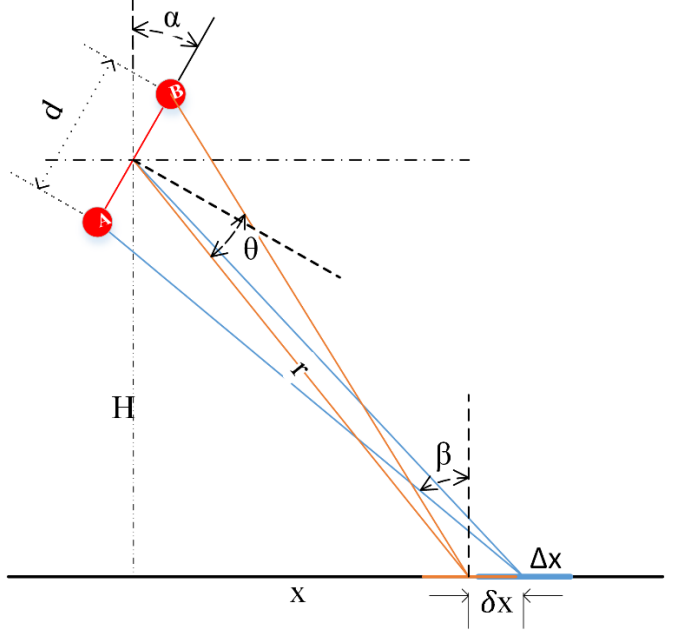


Figure 9 Sliding footprint effect demonstration, where Δx is footprint size and δx is shift in the footprint.

The effective footprint used for bathymetry calculation is the common footprint seen by both receivers, and it contributes to a higher correlation coefficient. The non-common parts of the

footprint contribute to decorrelation noise, called spatial decorrelation [6].

The signal footprint length can be given by well-known equation:

$$\Delta x = \frac{cT}{2 \sin \beta} \quad (12)$$

The footprint shift can be expressed as [9]:

$$\delta x \approx \frac{d \sin(\theta)}{2 \sin(\beta)} \quad (13)$$

The equivalent SNR due to spatial decorrelation can be given by [6]:

$$SNR_{SL} \approx \frac{\Delta x - \delta x}{\delta x} \quad (14)$$

$$SNR_{SL} \approx \frac{cT}{d |\sin(\theta)|} - 1 \quad (15)$$

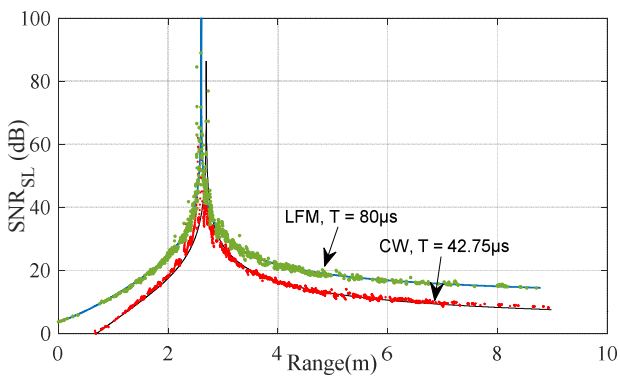


Figure 10: SNR_{SL} Spatial decorrelation over horizontal range taken with a depth of 1.5m. Model and field data compared with LFM and CW transmitted pulse

The overall SNR contributed by the sliding ladder effect (spatial decorrelation) can be improved slightly by using modulated signals. Another way to solve the problem is by estimating seabed depth and then applying an artificial delay between the receive signals to correct the shift.

c) Baseline Decorrelation

So far, we have considered that the backscattered echoes are the result of single point scatters, but that is not really the case. The final backscattered pattern of a footprint comes from an interference pattern from many distributed scatterers within the footprint. Now consider that this interference pattern is slightly different for two closely placed receive arrays, and that adds up in the final angle measurement error. This phenomenon is called angular decorrelation, also known as baseline decorrelation, and known as “glint” in the radar literature.

Jin and Tang [10] describe and discuss the baseline decorrelation effect. They express the SNR due to baseline decorrelation to the averaged cross-correlation coefficient of interferometry signals received at two receiver A and B separated by ‘d’.

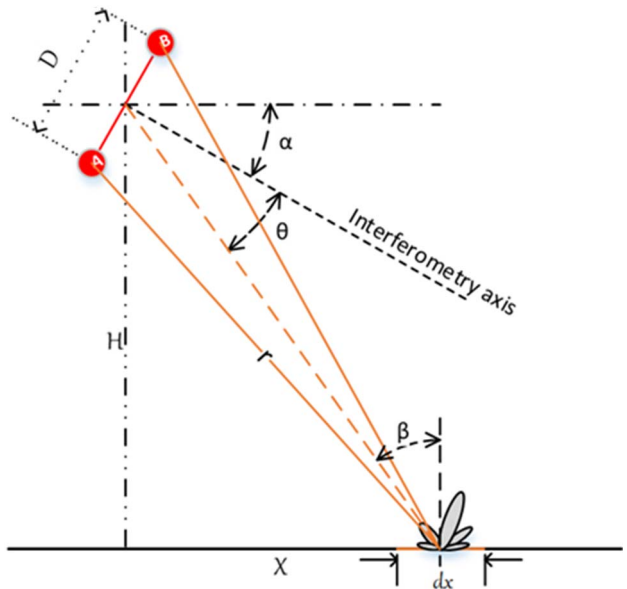


Figure 11: Interferometry setup considering target footprint response

The correlation coefficient is defined as:

$$\eta = \frac{|\langle S_a S_b^* \rangle|}{\sqrt{\langle S_a S_a^* \rangle \langle S_b S_b^* \rangle}} \quad (16)$$

Ref. [10], for our notation it can be written as:

$$\eta = \text{sinc} \left[\frac{kd}{\pi H} \frac{cT}{4} \sin \gamma \tan \gamma \cos(\gamma - \theta) \right] \quad (17)$$

Using (12)

$$\eta \approx \text{sinc} \left[\frac{kd}{2H} \Delta x \cos \beta \cos \theta \right] \quad (18)$$

The equivalent SNR can be computed from this baseline decorrelation coefficient.

$$SNR_{Angle} = \frac{\eta}{\eta - 1} \quad (19)$$

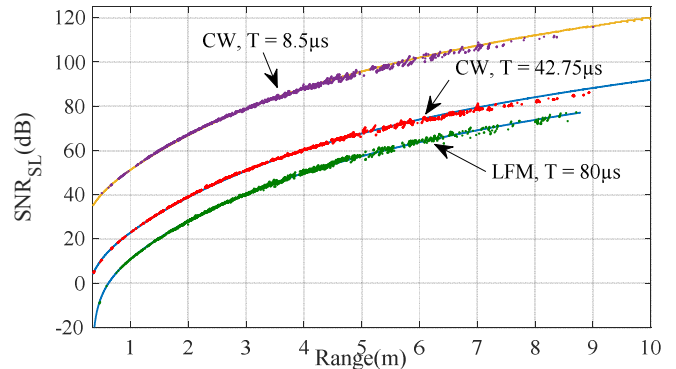


Figure 12 Baseline decorrelation effect; SNR to Horizontal Range

Concluding the results of Figure 12, an LFM pulse is the noisier than the two CW pulses when only considering the baseline decorrelation effect, which is mainly given by the sidelobe dominance in matched filter output.

d) Total SNR

The total signal to noise can be written as [8]:

$$SNR_{Total} = \frac{1}{\left(\frac{1}{SNR_{Additive}} + \frac{1}{SNR_{SL}} + \frac{1}{SNR_{Angle}} \right)} \quad (19)$$

Figure 13 represents the total SNR results for a CW system with pulse length $T = 42.75\mu s$ and an LFM signal with pulse length $T = 80\mu s$. The overall improvement is more dominant as we go further away in horizontal range. The improvement near nadir region is debatable and needs a different error model. Signals coming from the direction of the interferometry axis give maximum SNR in both cases. Now considering the standard deviation of phase difference measurements in Figure 14, wideband signals give better results in the far range. This is due to the dominance of baseline decorrelation in the area before the interferometry axis.

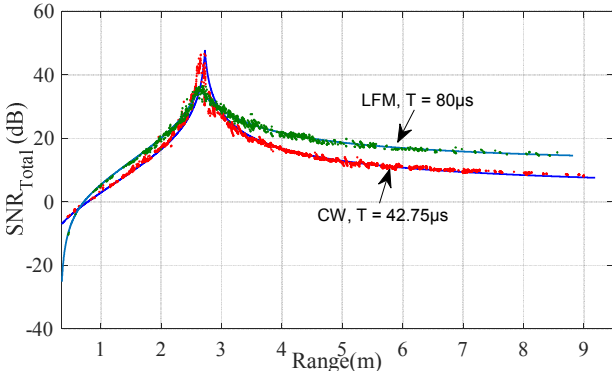


Figure 13 Total Signal to noise ratio considering Additive Noise, Sliding footprint and baseline decorrelation effect

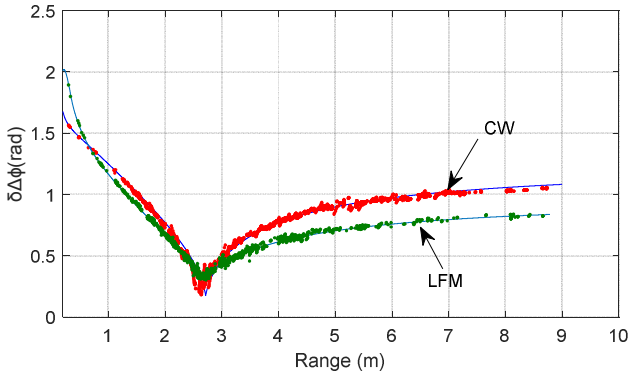


Figure 14 Phase difference standard deviation over horizontal range with LFM and CW transmitted pulses

III. IMPROVEMENT PROPOSAL

As discussed throughout this paper, the use of wideband signals should increase the overall performance of an interferometer, but the results are not as promising as hoped in the area before the zero-phase axis (interferometry axis). The main reason for this is the high sidelobes in the matched filter output when used with wideband signals. This can be related to the dominance of the baseline decorrelation effect, which is

proportional to the transmitted pulse length, and is larger in the case of modulated signals.

The results can be improved by adjusting with two parameters: transmitted pulse length (T) and bandwidth (B).

A. Pulse shape design

Tapering of the transmit signal is proposed by some researchers to reduce the sidelobes in the matched filter output [13]. The effective length of the envelope can be reduced by tapering the signal envelope from both ends. We have to trade off some of the energy as the main lobe of output signal gets wider. Use of shaped amplitude envelopes e.g. cosine, exponential... can help reduce this effect and it should be considered in future developments.

Frequency modulated transmitted signal is:

$$S(t) = a(t) * e^{2i\pi(f_ct+kt^2)} \quad (20)$$

By writing $a(t)$ as a function of time, we can get a desired shape of signal envelope. A square envelope consists the maximum energy, but the sharp edges of square envelope are smoothed by the transducer naturally. So, tapering the signal envelope till a certain point won't affect much the transmitted energy. But, over tampering with the envelope shape will reduce the transmitted energy, that will lead to reduced target range.

B. Filter Design

Windowing of the matched filter's reference signal can reduce the effect of sidelobe dominance, leading to improved SNR from baseline decorrelation.

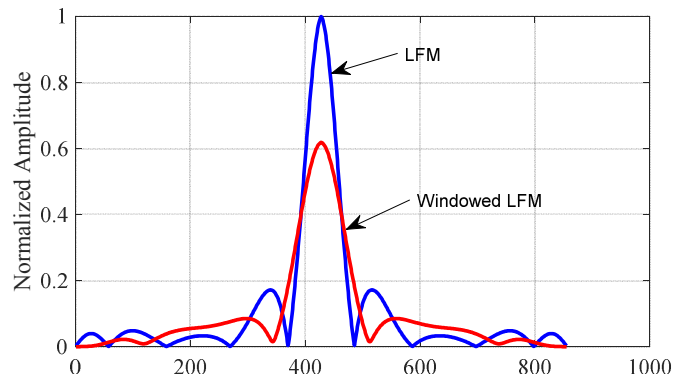


Figure 15 Auto-correlation of LFM pulse (Blue) and LFM pulse after applying Hamming window (Red)

IV. CONCLUSION

In this paper, we gave a quick introduction to the interferometric method of bathymetry measurement and the bathymetric errors associated with various signal processing methods. We justified the need for using wideband signals to achieve a wide swath and high-resolution bathymetry but also the drawbacks associated with them.

The following were discussed:

- High-resolution bathymetry is desired, but conventional narrowband CW systems face a high

range-resolution trade-off. Pulse compression techniques with wideband signals give a good alternative to achieve a long range with high spatial resolution.

- Interferometers face phase ambiguity problems while using a wide baseline and ambiguous phase measurements while using a short baseline ($< \lambda/2$). A successive computation of angle using Vernier technique is done to overcome the phase ambiguity problem.
- Additive noise can be reduced significantly by using a modulated transmitted signal. Matched filtering at the receive end gives a processing gain given by time – bandwidth product (BT).
- SNR due to sliding footprint or spatial decorrelation can be improved slightly using LFM pulses but the benefits mostly apply to the seabed beyond the interferometry axis. One way to remove the sliding footprint effect is to estimate the seabed depth and then delay the receive signals to correct the shift of footprint.
- The major problem of using wideband signals is the baseline decorrelation effect. This is mainly due to sidelobe dominance in the matched filter output. The wider the transmitted energy envelope, the more decorrelation between the interferometry signals. A few ideas are given to reduce the baseline decorrelation effect, e.g. tapering the transmitted signal envelope, and improving the matched filter designs. But in both cases, we have to trade off some of the energy, as it widens the matched filter's main lobe.

The techniques explored in this paper mostly have an effect after the zero-phase line (the interferometric axis). A more accurate error model for the nadir region should be given in future. Future developments will include a merit-based assessment of different transmit pulse sequence designs and improved filtering techniques to reduce the baseline decorrelation effect.

REFERENCES

- [1] M.J.P. Heaton and W.G. Haslett, "Interpretation of Lloyd mirror in sidescan sonar", Proc. Soc. Underwater Tech., vol. 1, no. 1, pp. 24-38, 1971.
- [2] P.N. Denbigh, "A bathymetric sidescan sonar", In proc. Ultrasonics Int. '79 Conf., 1979
- [3] ITER Systems Product Document, "Bathyswath-2 Technical Information", Sep. 2016
- [4] X. Lurton, An Introduction to Underwater Acoustics, Springer, 2003.
- [5] C. Sintès , " Strategies for unwrapping multisensors interferometric side scan sonar phase", OCEANS 2000 MTS/IEEE Conference and Exhibition, vol. 3, pp. 2059-2065, Sept. 2000
- [6] X.Lurton, "Swath Bathymetry Using Phase Difference: Theoretical Analysis of Acoustical Measurement precision", IEEE Journal of Oceanic Engineering, Vol.25, NO. 3, pp. 351-363, July 2000
- [7] Philip N Denbigh, "Swath Bathymetry: Principles of Operation and an Analysis of Errors", in IEEE Journal of Oceanic Engineering, Vol.14, pp. 289-298, Oct. 1989
- [8] X. Lurton, "Theoretical Modelling of Acoustical Measurment Accuracy for Swath Bathymetric Sonars", International Hydrographic Review, vol. 4 No. 2 ,2003
- [9] John S. Bird, Geoff K. Mullins, "Analysis of Swath Bathymetry Sonar Accuracy", IEEE Journal of Oceanic Engineering, vol 30, no.2, pp. 372–390, April 2005.
- [10] G. Jin and D. Tang, "Uncertainties of differential phase estimation associated with interferometric sonars", IEEE Journal of Oceanic Engineering, vol 21, no.1, pp. 53–63, Jan. 1996.
- [11] P. Vincent, F. Maussang, X. Lurton, C. Sintès, R. Garello, "Impact of FM pulse compression sidelobes on Multibeam Bathymetry Measurements", Proc. ECUA 2012, July 2012, Edinburgh, UK.
- [12] P. Vincent, F. Maussang, X. Lurton, C. Sintès, R. Garello, "Bathymetry Degradation Causes for Frequency Modulated Multibeam Echo Sounders", OCEANS 2012 MTS/IEEE Conference, Oct. 2012, Hampton Roads, Virginia
- [13] Md. J. Alam, E. H. Huntington, M. R. Frater, "Relationship between length of the chirp and depth of the ocean in active sonar processing", IEEE 2013
- [14] S. Haykin, Adaptive Filter Theory, Prentice Hall, Englewood Cliffs, NJ, 1996